Front. Environ. Sci. Eng. 2013, 7(3): 382–387
DOI 10.1007/s11783-013-0504-5

RESEARCH ARTICLE

Removal of rhodamine B from aqueous solution by $BiPO_4$ hierarchical architecture

Lei LI[1,2,3], Jian XU (✉)[1,2], Changsheng GUO[1,2], Yuan ZHANG[1,2]

1 State Key Laboratory of Environmental Criteria and Risk Assessment, Chinese Research Academy of Environmental Sciences, Beijing 100012, China
2 Laboratory of Riverine Ecological Conservation and Technology, Chinese Research Academy of Environmental Sciences, Beijing 100012, China
3 Jinan Environmental Protection Planning & Design Research Institute, Jinan 250001, China

Abstract Hexahedron-like $BiPO_4$ microcrystals were sucessfully synthesized via a template-free hydrothermal method. The resulting samples were characterized by X-ray diffraction (XRD), field-emission scanning electron microscopy (FESEM), transmission electron microscopy (TEM) and UV–vis spectroscopy. The $BiPO_4$ samples were of pure monoclinic phase, and the initial amount of PO_4^{3-} during synthesis did not show obvious effect on the phase properties of the materials. The hexahedron-like $BiPO_4$ microcrystal had explicitly cut edges, and its thickness was about 1 μm. The photocatalytic performance of the $BiPO_4$ catalysts was evaluated by photodegradation of RhB under UV light irradiation with commerial Degussa P25 TiO_2 as reference. Compared with P25, the $BiPO_4$ catalysts displayed higher photocatalytic activity, with 98.7% of RhB degraded during 60-min experiment. Cost evaluation analysis was adopted to describe the energy consumption of the degradation process, and the results suggested the potential application of this material in the field of dye-contaminated wastewater treatment or environmental matrices remediation.

Keywords $BiPO_4$, photocatalysis, Rhodamine B, cost evaluation

1 Introduction

In the past few decades, heterogeneous photocatalysis of semiconductors has been applied to water-splitting and organic pollutant degradation under both UV and visible-light irradiation [1]. Many oxide semiconductors, including TiO_2, ZnO, SnO_2, CdS and CeO_2, have been studied as the photocatalyst to purify air, water and soil polluted with various hazardous chemicals [2,3]. Among diverse photocatalytic materials, TiO_2 is by far one of the most efficient and economical photocatalysts due to titania's abundance, nontoxicity, low-cost, unique optical-electronic properties and mild effect on the environment [4–6]. However, the fine powder of TiO_2 with high photocatalytic activity renders its application for industrial application, during which after reaction the small particles are too difficult to recover by traditional wastewater treatment techniques, and may re-pollute the water [7,8]. Moreover, owing to its relatively inefficient quantum yield and wide band gap energy, TiO_2 cannot be used in large scale industrial wastewater treatment [9].

Bismuth-based nanostructured materials ($BiWO_4$, BiOBr, Bi_2MoO_6, etc.) have recently attracted much attention because of their unique properties [10–13]. As an important multicomponent semiconductor, bismuth phosphate ($BiPO_4$) is widely studied as a good catalyst, orthophosphate ion-sensor, and separating agent [14]. Several methods have been applied to synthesize single-phase micro- or nano-scale $BiPO_4$ materials. $BiPO_4$ nanococoons and nanorods with different phases were successfully prepared by solvothermal method, and the materials proved the potential photoluminescence properties [15]. To controllably prepare the Bi salt nanocrystals, a method using high-temperature hydrolysis reaction was adopted for the synthesis of tailored $BiPO_4$ nanocrystals with enhanced photocatalytic performances [16]. However, to synthesize $BiPO_4$ materials by the facile method is still a challenge.

In the present work, $BiPO_4$ catalysts were prepared by a facile template-free hydrothermal method, using $Bi(NO_3)_3 \cdot 5H_2O$ as Bi source. Effect of the initial amount

Received August 28, 2012; accepted February 28, 2013

E-mail: xujian@craes.org.cn

of PO_4^{3-} during the preparation process was also explored. The physicochemical properties of the $BiPO_4$ samples were characterized by XRD, FESEM, TEM and UV–vis DRS techniques. The photocatalytic performance of the synthesized catalysts was investigated by the degradation of rhodamine B (RhB) under UV light irradiation. Furthermore, cost evaluation was applied to illustrate the potential environmental application of this material in the wastewater treatment processes.

2 Materials and methods

2.1 Chemicals and reagents

Bismuth nitrate pentahydrate ($Bi(NO_3)_3 \cdot 5H_2O$), sodium phosphate tribasic dodecahydrate ($Na_3PO_4 \cdot 12H_2O$), HNO_3 and rhodamine B (RhB) were in analytical grade and purchased from Tianjin Chemical Reagent Corporation, China. P25 TiO_2 was purchased from Degussa Corporation (anatase:rutile = 80∶20, particle size of 21 nm, BET area of 50 $m^2 \cdot g^{-1}$). Ultrapure water was prepared by a Milli-Q water purification system (Millipore, Bedford, MA, USA). All the chemicals were used as received without further purification.

2.2 Synthesis of $BiPO_4$ catalysts

$BiPO_4$ catalysts were prepared via a facile hydrothermal method with $Bi(NO_3)_3 \cdot 5H_2O$ as Bi source. In a typical procedure, a quantity of 1.14 g $Na_3PO_4 \cdot 12H_2O$ were dissolved in 20 mL ultrapure water, then 20 mL of 0.15 $mol \cdot L^{-1}$ $Bi(NO_3)_3 \cdot 5H_2O$ stock solution was added dropwisely with vigorous stirring. The obtained solution was magnetically stirred for 30 min, and transferred to a 50 mL Teflonlined autoclave vessel, which was maintained in the oven at 180°C for 72 h. After naturally cooling down, the products were centrifuged, and the precipitates were rinsed thoroughly with distilled water and ethanol several times. The samples were then dried in the oven at 60°C for 5 h. The above molar ration of PO_4^{3-} to Bi^{3+} was 1:1, and the sample was denoted as $BiPO_4$-B. The effect of the amount of PO_4^{3-} was further investigated, and the corresponding molar ratios of PO_4^{3-} to Bi^{3+} were adjusted to 0.7∶1 and 1.3∶1, with the resulting samples named as $BiPO_4$-A and $BiPO_4$-C, respectively.

2.3 Characterization

The phase structure of $BiPO_4$ catalysts was recorded by a diffractometer (Max-2500, Rigaku D, Japan) using Cu Kα radiation (λ = 1.54178 Å). The morphologies and sizes of the samples were determined by field-emission scanning electron microscopy (FESEM, FEI Nanosem 430, China) and transmission electron microscopy (TEM, JEM-100CX II, Japan). The optical properties of the samples were evaluated by a spectrophotometer (UV-3600, Shimadzu, Japan) equipped with integrating spheres using $BaSO_4$ as reference at room temperature.

2.4 Photocatalytic experiments

The photocatalytic degradation experiments were performed in a photochemical reactor (XPA-2, Nanjing Xujiang Machinery Factory, Nanjing, China). A 100 W mercury lamp (Institute of Electric Light Source, Beijing) was used as UV light source, which was positioned in the middle of the cylindrical quartz cold trap. The whole system was cooled by circulating water and maintained at room temperature. In each experiment, an amount of 0.2 g catalyst was added to the reaction system containing 200 mL of 0.1 $mol \cdot L^{-1}$ RhB. The resulting suspension was magnetically stirred in darkness for 30 min to achieve adsorption–desorption equilibrium. After turning on the light, aliquots of 4 mL reaction solution were sampled at predetermined time intervals. The concentration of RhB was determined by UV–vis absorption spectra (Shimadzu UV1600) at wavelength of 554 nm with the supernatant pre-centrifuged at 3000 rpm for 10 min. The conversion of RhB was calculated by the following equation:

$$Conversion(\%) = 1 - \frac{C_t}{C_0}, \quad (1)$$

where, C_0 and C_t were the initial adsorption equilibrium concentration of RhB and the reaction concentration at time t (min), respectively.

3 Results and discussion

3.1 XRD analysis

Figure 1 presented the XRD patterns of catalysts prepared at various molar ratios of $Na_3PO_4 \cdot 12H_2O$ to $Bi(NO_3)_3 \cdot 5H_2O$. The XRD images were well indexed to the crystallized pure monoclinic phase $BiPO_4$ with lattice parameters of $a = b = 6.982$, $c = 6.476$ Å (JCPDS No. 15-0767) (its standard image was shown at the bottom of Fig. 1), without other characteristic peaks observed, indicating the high purity of obtained $BiPO_4$ catalysts. The intense and sharp diffraction peaks indicated the high degree of crystallinity of the $BiPO_4$ catalysts. Comparison of the XRD images of $BiPO_4$-A, $BiPO_4$-B and $BiPO_4$-C showed no obvious changes for positions or intensities of the diffraction peaks, suggesting that the initial amount of PO_4^{3-} did not influence the phase properties of the $BiPO_4$ catalysts. In the following parts, $BiPO_4$-B (molar ratios of PO_4^{3-} to Bi^{3+} at 1:1) was chosen as model catalyst and denoted as $BiPO_4$.

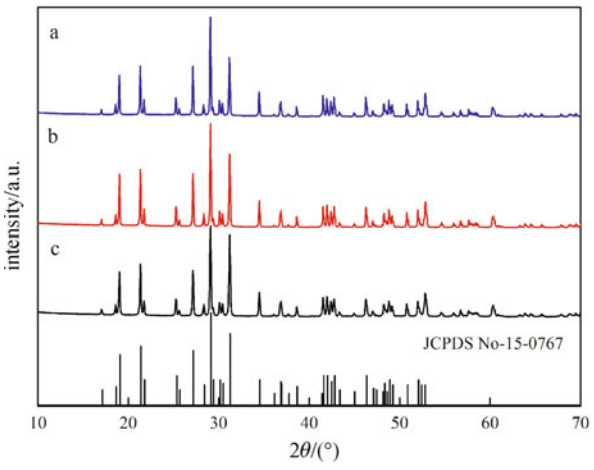

Fig. 1 XRD patterns of the synthesized $BiPO_4$ catalysts with the molar ratios of $Na_3PO_4 \cdot 12H_2O$ to $Bi(NO_3)_3 \cdot 5H_2O$ at 0.7:1 (a), 1:1 (b) and 1.3:1 (c), respectively

3.2 Morphology

The morphologies and sizes of the prepared catalysts were depicted by SEM and TEM analysis (Fig. 2). The fabricated $BiPO_4$ samples were hexahedron-like microcrystals with explicit cut edges. The thickness of the $BiPO_4$ microcrystals was about 1 μm. Compared with P25 TiO_2 of 21 nm in size, the as-synthesized $BiPO_4$ catalysts may be easily separated from the photocatalytic reaction system via self-sedimentation, which is beneficial for its practical industrial application. Some faces of the samples were hollow (Fig. 2(b)), which can facilitate the diffusion of reactants/intermediates during the photocatalytic process. TEM picture of the $BiPO_4$ samples (Fig. 2(c)) confirmed the explicit cut edges of the prepared catalysts. The regular square diffraction spot array of SAED pattern (inset in Fig. 2(c)) confirmed the well crystallized single-phase of $BiPO_4$ samples, which was consistent with the results of XRD analysis.

3.3 Optical ability

For a semiconductor photocatalyst, the optical absorption property determines its electronic structure and migration of the light-induced electrons and holes, which plays important roles during the photocatalytic process [17]. Optical absorption ability of $BiPO_4$ was determined by the UV-vis spectroscopy, and the corresponding result was displayed in Fig. 3. The intense absorption band with a steep edge of the spectrum indicated that the absorption in the UV region was due to the intrinsic band gap transition instead of the transition from the impurity levels [18]. The $BiPO_4$ samples showed obvious absorption in the UV light region with an absorption edge of 310 nm. For a crystalline semiconductor, the optical absorption near the band edge follows the following equation:

$$\alpha h\nu = A(h\nu - E_g)^{\frac{n}{2}}, \tag{2}$$

where, α, ν, E_g and A are the absorption coefficient, the light frequency, the band gap, and a constant, respectively [19]. Thus, the band gap energy of $BiPO_4$ samples was estimated to be *ca.* 4.0 eV. This was in agreement with the previous reported values [20].

3.4 Photocatalytic degradation of RhB by $BiPO_4$

Figure 4 illustrated the RhB removal efficiencies as a function of reaction time with Degussa P25 TiO_2 as reference. Preliminary experiments indicated that adsorption-desorption equilibrium between RhB and the catalysts was achieved after 30 min continuous stirring in the dark. The removal efficiencies of RhB by $BiPO_4$ and P25 were 98.7% and 93.8%, respectively, after 60 min irradiation. Photodegradation of RhB versus the irradiation time follows the pseudo first-order kinetic model:

$$-\ln\frac{C_t}{C_0} = k_{app}t, \tag{3}$$

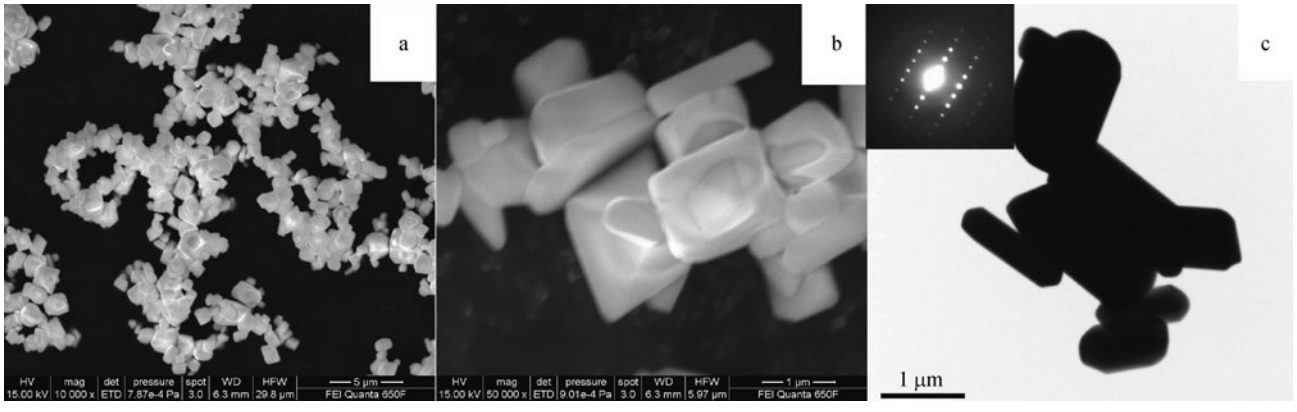

Fig. 2 SEM (a and b) and TEM (c) images of the prepared $BiPO_4$ catalysts

where C_0 and C_t are the initial RhB concentration and concentration at reaction time t (min), respectively; k_{app} is the reaction rate constant. The parameter k_{app} can be determined by the gradient of the line of $\ln(C_t/C_0)$ versus time t. In this study the reaction rate constants k_{app} for $BiPO_4$ and P25 were calculated to be 0.071 and 0.043 min^{-1}, respectively. The synthesized $BiPO_4$ powders proved to be efficient for RhB removal from solution, and the obtained reaction rate constants k_{app} were comparable to reported values by other researchers with Bi_2WO_6, Bi_2MoO_6, or highly ordered macro-mesoporous anatase TiO_2 film [21,22]. Compared with P25 TiO_2, the higher k value of $BiPO_4$ suggested the significantly superior photocatalytic activity of the synthesized $BiPO_4$, which was probably ascribed to the following two reasons. First, the relatively high crystallinity of the $BiPO_4$ sample meant the few defects in the photocatalysts, which may serve as recombination centers for the photoexcited electron-hole pairs and result in the superior photocatalytic activity of $BiPO_4$ catalyst [23]. Secondly, $BiPO_4$ semiconductors are of high position of the valence band and high separation efficiency of electron-hole pairs [24], which leads to a reduction in the probability of the recombination of e^-/h^+ pairs and an increase of the charge transfer, facilitating the photocatalytic process.

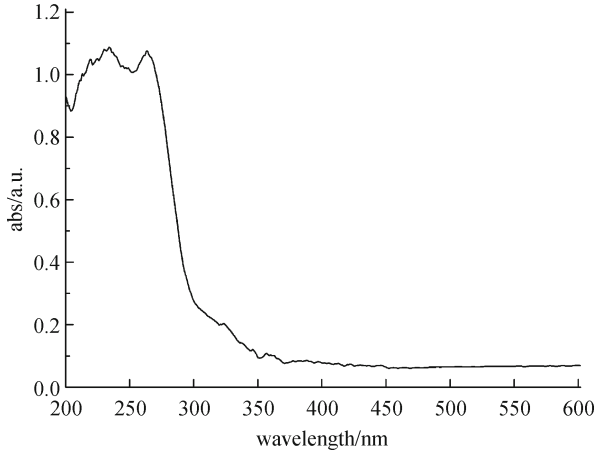

Fig. 3 UV–vis absorption spectra of the obtained $BiPO_4$ catalysts

The temporal changes of RhB with respect to $BiPO_4$ were likely caused by the de-ethylation and efficient decomposition of RhB in a stepwise manner [25]. The photocatalytic process was initiated by the photoabsorption of light, which generated electrons (e^-) and holes (h^+). The holes subsequently reacted with the molecular H_2O to yield HO· radicals. Simultaneously, the newly formed electrons reacted with the adsorbed molecular oxygen and produced the superoxide radical anion O_2^-, which was further transformed to the ·OOH radicals [26]. The existing active oxygen radicals (HO·, ·OOH) oxidized the adsorbed RhB by the attack of the N-ethyl group and led to the stepwise de-ethylation, producing a series of *N*-deethylated intermediates. During this process, the original *N*,*N*,*N*′,*N*′,-tetraethylated rhodamine molecule (λ_{max} = 554 nm) was gradually transformed to *N*,*N*,*N*′-tri-ethylated rhodamine (λ_{max} = 539 nm), *N*,*N*′-di-ethylated rhodamine (λ_{max} = 522 nm), N-ethylated rhodamine (λ_{max} = 510 nm), and finally to rhodamine (λ_{max} = 498 nm) [27–29]. Parallel to that, destruction of the dye chromophore ring structure took place, and the dye molecules were degraded with the extending irradiation time [28]. With the prolonged UV-vis illumination, the whole processes ended in the mineralization of the formed intermediates to small molecules, such as NH_4^+, CO_2, and H_2O.

3.5 Environmental applications

This study demonstrated high photocatalytic performance of the synthesized $BiPO_4$ catalysts on the degradation of RhB in aqueous solution under UV light irradiation. The half-lives of corresponding contaminants were calculated from the equation $t_{1/2} = \ln 2/k_{app}$, and results were summarized in Table 1. By comparison of the data from photolysis of RhB, both P25 and $BiPO_4$ could significantly shorten the $t_{1/2}$, and their $t_{1/2}$ values were in the same order of magnitude.

The electrical energy per order (E_{EO}) is proposed to assess the electrical energy required to remove unit mass of pollutant. The E_{EO} is defined as the number of kWh of electrical energy required to reduce the concentration of a pollutant by 1 order of magnitude (90%) in 1 m^3 of the contaminated water, and the equation is expressed as follows [3]:

$$E_{EO} = \frac{P \times t \times 1000}{V \times 60 \times \ln(C_0/C)}, \quad (4)$$

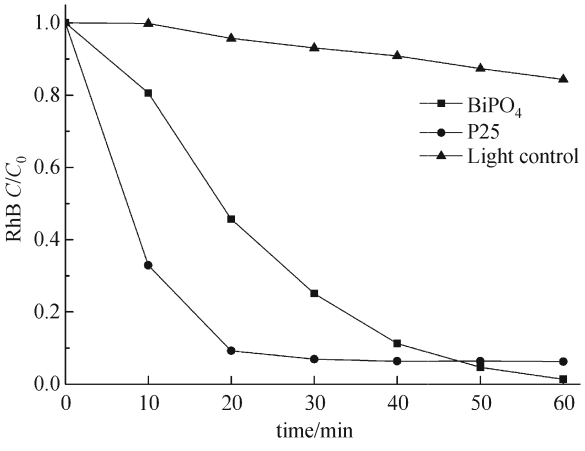

Fig. 4 Photocatalytic degradation of RhB (1.0 mg·L^{-1}) by different catalysts under UV light irradiation. Initial RhB concentration was 10.0 mg·L^{-1}, and catalyst dosage was 1.0 g·L^{-1}

Table 1 Apparent rate constants, half-life and E_{EO} for the degradation of RhB in the reaction systems

	k/ min^{-1}	half-life/min	E_{EO} /(kW h· m^{-3} $order^{-1}$)
photolysis	0.0057	121.60	24.367
P25 TiO_2	0.043	16.12	0.323
$BiPO_4$	0.071	9.76	0.014

$$\ln(C_0/C) = k_{app}t. \quad (5)$$

where, P is the rated power (kW) of the advanced oxidation process system, t is the irradiation time (h), V is the volume (L) of the water in the reactor, C_0 and C are the initial and final pollutant concentrations and k is the pseudo-first-order rate constant (min^{-1}) representing the decay of the pollutant concentration. The calculated E_{EO} values (Table 1) by P25 and $BiPO_4$ catalysts showed the same trend as $t_{1/2}$ values. The low energy consumption by synthesized $BiPO_4$ catalysts demonstrated that less energy was needed for keeping the high degradation efficiency in the $BiPO_4$ system. These results imply that the synthesized $BiPO_4$ catalysts could efficiently degrade organic dye compounds, suggesting the promising prospect in the application of $BiPO_4$ catalysts for costly treating organic contaminants in wastewater.

4 Conclusions

Hexahedron-like monoclinic phase $BiPO_4$ was synthesized via a facile hydrothermal method with bismuth nitrate pentahydrate as Bi source. The band gap energy of the $BiPO_4$ samples was determined to be about 4.0 eV, which indicated the strong absorption in the UV region. Compared with P25 TiO_2, the superior photocatalytic performance of the prepared samples can be ascribed to the synthetic effect of its relative high crystallinity and high separation efficiency of electron-hole pairs. RhB was degraded in a stepwise manner in the $BiPO_4$/UV system, during which the reactive radicals (HO·, ·OOH) oxidized RhB by a stepwise de-ethylation process, and the whole reaction ended in the mineralization of the formed intermediates to small benign molecules. Cost evaluation results demonstrated the potential application of the obtained $BiPO_4$ materials for the removal of organic dyes from wastewater.

Acknowledgements This work was funded by the National Natural Science Foundation of China (Grant No. 51208482).

References

1. Madhusudan P, Ran J R, Zhang J, Yu J G, Liu G. Novel urea assisted hydrothermal synthesis of hierarchical $BiVO_4$/$Bi_2O_2CO_3$ nanocomposites with enhanced visible-light photocatalytic activity. Applied Catalysis B: Environmental, 2011, 110: 286–295
2. Takeuchi M, Shimizu Y, Yamagawa H, Nakamuro T, Anpo M. Preparation of the visible light responsive N^{3-}-doped WO_3 photocatalyst by a thermal decomposition of ammonium paratungstate. Applied Catalysis B: Environmental, 2011, 110: 1–5
3. Esen B, Yumak T, Sınağ A, Yıldız T. Investigation of photocatalytic effect of SnO_2 nanoparticles synthesized by hydrothermal method on the decolorization of two organic dyes. Photochemistry and Photobiology, 2011, 87(2): 267–274
4. Farhangi N, Chowdhury R R, Medina-Gonzalez Y, Ray M B, Charpentier P A. Visible light active Fe doped TiO_2 nanowires grown on graphene using supercritical CO_2. Applied Catalysis B: Environmental, 2011, 110: 25–32
5. Guo C S, Xu J, Zhang Y, He Y. Hierarchical mesoporous TiO_2 microspheres for the enhanced photocatalytic oxidation of sulfonamides and their mechanism. RSC Advances, 2012, 2(11): 4720–4727
6. Wang S H, Wang K H, Jehng J, Liu L C. Preparation of TiO_2/MCM-41 by plasma enhanced chemical vapor deposition method and its photocatalytic activity. Frontiers of Environmental Science & Engineering, 2012, 6(3): 304–312
7. Acosta-Silva Y J, Nava R, Hernández-Morales V, Macías-Sánchez S A, Gómez-Herrera M L, Pawelec B. Methylene blue photodegradation over titania-decorated SBA-15. Applied Catalysis B: Environmental, 2011, 110: 108–117
8. Ge M, Guo C S, Zhu X W, Ma L L, Han Z N, Hu W, Wang Y Q. Photocatalytic degradation of methyl orange using ZnO/TiO_2 composites. Frontiers of Environmental Science & Engineering in China , 2009, 3(3): 271–280
9. Wang D J, Xue G L, Zhen Y Z, Fu F, Li D S. Monodispersed Ag nanoparticles loaded on the surface of spherical Bi_2WO_6 nanoarchitectures with enhanced photocatalytic activities. Journal of Materials Chemistry, 2012, 22(11): 4751–4758
10. Wang C Y, Zhang H, Li F, Zhu L Y. Degradation and mineralization of bisphenol A by mesoporous Bi_2WO_6 under simulated solar light irradiation. Environmental Science & Technology, 2010, 44(17): 6843–6848
11. Xu J, Meng W, Zhang Y, Li L, Guo C S. Photocatalytic degradation of tetrabromobisphenol A by mesoporous BiOBr: Efficacy, products and pathway. Applied Catalysis B: Environmental, 2011, 107(3–4): 355–362
12. Zhang L W, Xu T G, Zhao X, Zhu Y F. Controllable synthesis of Bi_2MoO_6 and effect of morphology and variation in local structure on photocatalytic activities. Applied Catalysis B: Environmental, 2010, 98(3–4): 138–146
13. Guo C S, Xu J, Wang S F, Li L, Zhang Y, Li X C. Facile synthesis and photocatalytic application of hierarchical mesoporous Bi_2MoO_6 nanosheet-based microspheres. CrystEngComm, 2012, 14(10): 3602–3608

14. Geng J, Hou W H, Lv Y N, Zhu J J, Chen H Y. One-dimensional $BiPO_4$ nanorods and two-dimensional BiOCl lamellae: fast low-temperature sonochemical synthesis,characterization, and growth mechanism. Inorganic Chemistry, 2005, 44(23): 8503–8509
15. Xue F, Li H B, Zhu Y C, Xiong S L, Zhang X W, Wang T T, Liang X, Qian Y T. Solvothermal synthesis and photoluminescence properties of $BiPO_4$ nano-cocoons and nanorods with different phases. Journal of Solid State Chemistry, 2009, 182(6): 1396–1400
16. Pan C S, Zhu Y F. Size-controlled synthesis of $BiPO_4$ nanocrystals for enhanced photocatalytic performance. Journal of Materials Chemistry, 2011, 21(12): 4235–4241
17. Ge M, Li J W, Liu L, Zhou Z. Template-free synthesis and photocatalytic application of rutile TiO_2 hierarchical nanostructures. Industrial and Engineering Chemistry Research, 2011, 50(11): 6681–6687
18. Wang C Y, Zhu L Y, Song C, Shan G Q, Chen P. Characterization of photocatalyst $Bi_{3.84}W_{0.16}O_{6.24}$ and its photodegradation on bisphenol A under simulated solar light irradiation. Applied Catalysis B: Environmental, 2011, 105(1–2): 229–236
19. Tian G H, Chen Y J, Zhou W, Pan K, Dong Y Z, Tian C G, Fu H G. Facile solvothermal synthesis of hierarchical flower-like Bi_2MoO_6 hollow spheres as high performance visible-light driven photocatalysts. Journal of Materials Chemistry, 2011, 21(3): 887–892
20. Li G F, Ding Y, Zhang Y F, Lu Z, Sun H Z, Chen R. Microwave synthesis of $BiPO_4$ nanostructures and their morphology-dependent photocatalytic performances. Journal of Colloid and Interface Science, 2011, 363(2): 497–503
21. Belver C, Adán C, Fernández-García M. Photocatalytic behaviour of Bi_2MO_6 polymetalates for rhodamine B degradation. Catalysis Today, 2009, 143(3–4): 274–281
22. Zhao J Q, Wan P, Xiang J, Tong T, Dong L, Gao Z N, Shen X Y, Tong H. Synthesis of highly ordered macro-mesoporous anatase TiO_2 film with high photocatalytic activity. Microporous and Mesoporous Materials, 2011, 138(1–3): 200–206
23. Wang Y W, Zhang L Z, Deng K J, Chen X Y, Zou Z G. Low temperature synthesis and photocatalytic activity of rutile TiO_2 nanorod superstructures. Journal of Physical Chemistry C, 2007, 111(6): 2709–2714
24. Pan C S, Zhu Y F. New type of $BiPO(_4)$ oxy-acid salt photocatalyst with high photocatalytic activity on degradation of dye. Environmental Science and Technology, 2010, 44(14): 5570–5574
25. Guo C S, Xu J, He Y, Zhang Y, Wang Y Q. Photodegradation of rhodamine B and methyl orange over one-dimensional TiO_2 catalysts under simulated solar irradiation. Applied Surface Science, 2011, 257(8): 3798–3803
26. Zheng Y, Duan F, Wu J, Liu L, Chen M Q, Xie Y. Enhanced photocatalytic activity of bismuth molybdates with the preferentially exposed {010} surface under visible light irradiation. Journal of Molecular Catalysis A Chemical, 2009, 303(1–2): 9–14
27. Bi J H, Wu L, Li J, Li Z H, Wang X X, Fu X Z. Simple solvothermal routes to synthesize nanocrystalline Bi_2MoO_6 photocatalysts with different morphologies. Acta Materialia, 2007, 55(14): 4699–4705
28. Wu T X, Liu G M, Zhao J C, Hidaka H, Serpone N. Photoassisted degradation of dye pollutants. V. self-photosensitized oxidative transformation of rhodamine B under visible light irradiation in aqueous TiO_2 dispersions. Journal of Physical Chemistry B, 1998, 102(30): 5845–5851
29. Zhao W, Chen C C, Li X Z, Zhao J C, Hidaka H, Serpone N. Photodegradation of sulforhodamine-B dye in platinized titania dispersions under visible light irradiation: influence of platinum as a functional co-catalyst. Journal of Physical Chemistry B, 2002, 106 (19): 5022–5028